Passive turbulent flamelet propagation

By Wm. T. Ashurst,[1] G. R. Ruetsch[2] AND T. S. Lund[2]

We analyze results of a premixed constant density flame propagating in three-dimensional turbulence, where a flame model developed by Kerstein *et al.* (1988) has been used. Simulations with constant and evolving velocity fields are used, where peculiar results were obtain from the constant velocity field runs. Data from the evolving flow runs with various flame speeds are used to determine two-point correlations of the fluctuating scalar field and implications for flamelet modeling are discussed.

1. Introduction

For some applications, it is useful to consider the premixed flame structure as unchanged by turbulence and to cast the problem as a flamelet moving through the flow with a known density jump (Liñán & Williams, 1993). A further assumption is to ignore the density change and consider passive flamelet propagation. We find that these constant-density flames do reveal possible mechanisms of turbulent flame propagation (Ashurst, 1994). Therefore, the flamelet assumption has been exploited in order to decouple the complexity of chemistry from that of turbulence. To investigate flame stability, Markstein wrote a flame evolution equation in 1964, but lacking a computer, he was restricted to a stability analysis. Markstein's notation was f for a flame with volume expansion; while a passive formulation has acquired the letter G; we distinguish between these flamelet models by using f when volume expansion is considered and G when it is not. The special initial condition formulated by Kerstein *et al.* (1988) is $G = x$ for the evolution equation

$$\frac{\partial G}{\partial t} + \mathbf{u} \cdot \nabla G = S_L |\nabla G| \tag{1}$$

where the right side describes Huygens' propagation with S_L as the burning velocity. This nonlinear term makes the initial condition very special: it provides a connection between flame area and the gradient of G. The scalar gradient corresponds to the flame surface density, that is, flame area per unit volume. In this passive formulation any level surface represents a flame and spatial derivatives of G define the geometry of that particular surface, thus the actual magnitude of G is not important. This formulation allows a numerical simulation which follows Damköhler's idea: creation of flame area by turbulent motion causes an increased consumption rate. Now, with the passage of fifty years, the computer can easily determine passive flame area within a turbulence simulation and, when the motion is forced, a statistically steady propagation is achieved.

1 Combustion Research Facility, Sandia National Laboratories, Livermore, CA
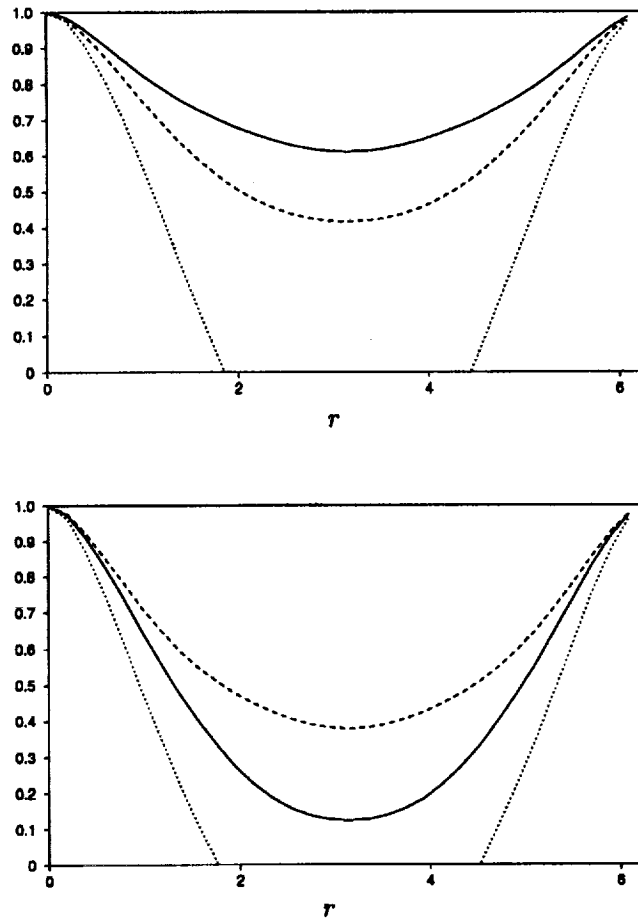2 Center for Turbulence Research

FIGURE 1.   Autocorrelations $_iR_{11}$ (top) and $_iR_{22}$ (bottom) for $u' = S_L/2$.
———— $:i = 1$, ---- $:i = 2$, and ······· $:i = 3$.

2. Summer objective

The initial suggestion for the Summer Program was motivated by the previous work of Lund & Rogers (1994) which examined the eigenvalues of the strain-rate tensor in forced, homogeneous, isotropic turbulence. Their velocity fields, on meshes up to 256^3, could be used as a frozen flow in which the propagation of the scalar G would be done, and thereby, obtain the G statistics at a smaller cost. This suggestion did not work. The frozen flow created very large distortions in the G level surfaces, so large that a single surface was connected across the periodic system length. This occurred because the amplitude of flame distortion in a frozen flow is proportional to the rms velocity of the velocity mode (Ashurst *et al.*, 1988) and the lowest modes have the largest energy content in these forced simulations. Since any level surface represents a flame in this passive model, the large distortions
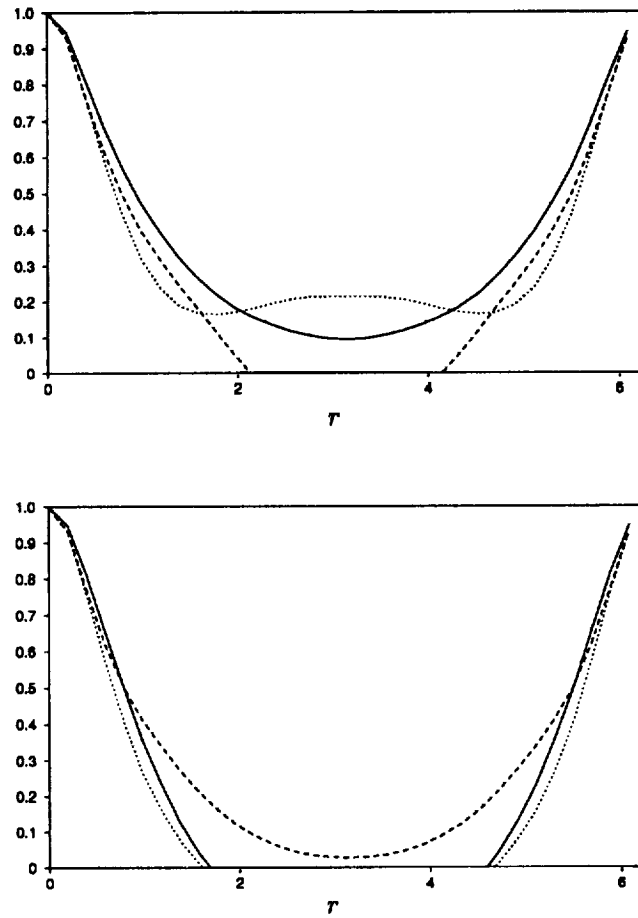
FIGURE 2. Autocorrelations $_iR_{11}$ (top) and $_iR_{22}$ (bottom) for $u' = 2S_L$. The line types follow the convention in Fig. 1.

correspond to flames interacting with their own periodic image and this is not desirable. The distortion amplitude is reduced when the flow has a time variation, and so evolution of both the velocity field and the scalar G field has been done with 32^3 systems.

Previous G field simulations have been done with finite-difference techniques where the truncation error combined with grid-resolution suppresses large gradients in the G field. These large gradients correspond to a cusp in a G surface, and the cusps are formed by the Huygens' propagation mechanism. Cusp formation and the pseudo-spectral solution technique are not compatible, and so a hyperdiffusivity term was added to the dynamical equation of the form $D\nabla^4 G$ with $D = 4\nu$.
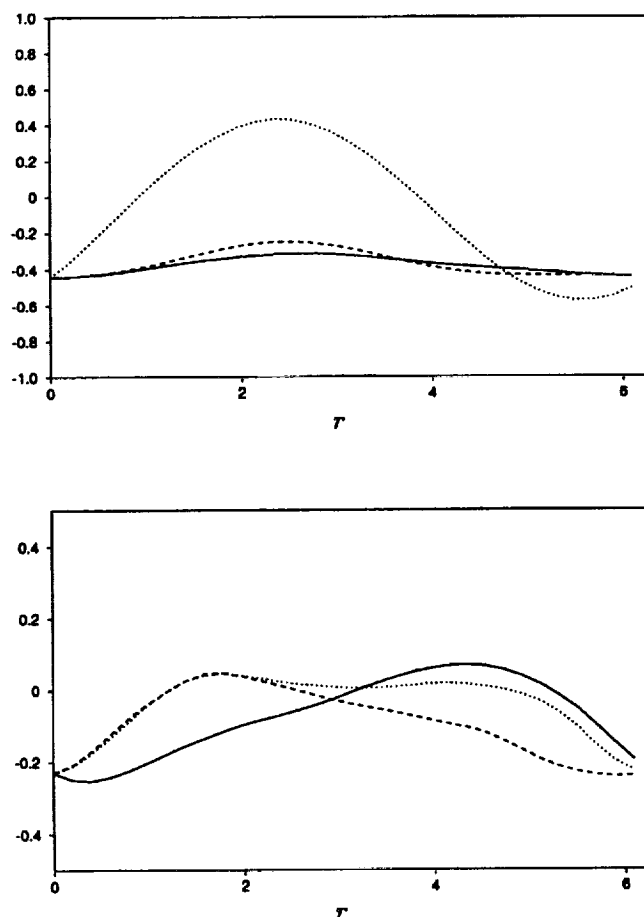
FIGURE 3. Cross-correlations $_iR_{12}$ for $u' = S_L/2$ (top) and $u' = 2S_L$ (bottom). The line types follow the convention in Fig. 1.

3. Isotropic propagation

Are the scalar fluctuations of G isotropic? Peters (1992) considers an ensemble of flamelets travelling from all directions into a spatial domain, and so within this domain the fluctuations are assumed to be isotropic. Thus, the well-developed analysis of isotropic, homogeneous turbulence may be applied to the geometry of these flamelets. The geometry is related to the scalar fluctuations as a consequence of the initial condition that $G = x$. The fluctuations correspond to the negative of the flame displacement from the transverse plane associated with that particular flame: use $g' = G - x$, and by adding a constant so that $G = 0$, we obtain g' as the negative displacement from the mean flame location where $G = 0$. The additive constant can be done for any plane normal to the mean propagation direction, and thereby we relate g' values to flame displacement from a transverse plane.
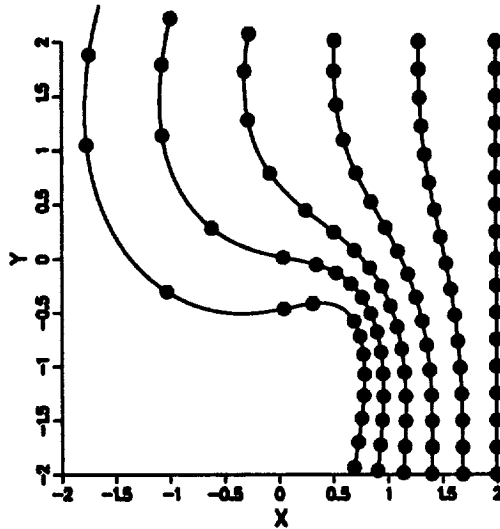
FIGURE 4. Passive front propagation through the swirling flow created by a Gaussian distribution of vorticity, the maximum swirl velocity is $0.8S_L$ and the spatial unit is 4η with a time interval between flame images of $2\eta/S_L$. The filled circles are points which are moved in the local flame normal direction, and the change in their spacing with time indicates the stretching of the flame surface.

To examine this issue with the numerical simulations, two scalar fields were computed within the domain: G_1 with mean gradient in the x direction and G_2 with a gradient in the y direction. For analysis of the scalar fluctuations, the mean gradient is removed ($g_1 = G_1 - x + x_o$ and $g_2 = G_2 - y + y_o$) and the values of x_o and y_o are determined so that g_1 and g_2 have a zero mean volume average. Division by their rms values provides autocorrelations with value of unity for zero separation. We can define a general two-point correlation as:

$$_iR_{jk}(r) = \overline{g_j(\mathbf{x})g_k(\mathbf{x} + r\mathbf{e}_i)}$$

where autocorrelations refer to instances where $j = k$ and cross-correlations otherwise. Autocorrelations for simulations with $u' = S_L/2$ and $u' = 2S_L$ are shown in Figs. 1 and 2. This data in these figures are taken from a single realization of the scalar field. Due to the limited sampling the correlations are not fully converged, but do exhibit dominant trends which we now discuss.

When $u' = S_L/2$, the autocorrelation is larger in the direction of the imposed mean gradient (for either g_1 or g_2). Therefore, the Huygens' propagation dominates over the distortions created by the velocity fluctuations and the passive scalar

fluctuations do have a directional bias. However, when $u' = 2S_L$, then the autocorrelations no longer show as strong a directional dependence.

The cross correlations indicate a negative value for zero separation and an asymmetric nature with respect to direction of the separation, see Fig. 3. We now speculate on why this is so. In Fig. 4, we present flame shapes created by passive propagation through the swirling flow created by a Gaussian distribution of vorticity. The propagation is from right to left, corresponding to a scalar G field with mean gradient increasing towards positive x. To the right, before the flame interacts with the vortex, the straight flame implies that $g' \sim 0$ along that flame surface. On the left side, after the interaction, the flame is distorted so that above the vortex center $g' > 0$ and below the center $g' < 0$. Hence, the swirling flow combined with Huygens' propagation creates asymmetric flame shapes. Taking Fig. 4 and rotating it a quarter of a turn counter-clockwise gives the solution for the scalar field G_2 which has its mean gradient towards $+y$. Now the cross-correlation between G_1 and G_2, using g'_1 and g'_2, has a significant contribution in only one quadrant, the lower-left quadrant in Fig. 4, where $g'_1 < 0$ and $g'_2 > 0$ producing a negative cross-correlation for zero separation.

4. Future work

Visualization of the intense vorticity and its relationship to flame area will be one aspect of future work. In previous work, Ruetsch & Maxey (1992) found that intense passive scalar gradients occur between vortical regions; will the same structure occur in a propagating, passive scalar field?

<div align="center">REFERENCES</div>

ASHURST, WM. T., SIVASHINSKY, G. I. & YAKHOT, V. 1988 Flame front propagation in nonsteady hydrodynamic fields. *Combust. Sci. & Tech.* **62**, 273-284.

ASHURST, WM. T. 1994 Modeling turbulent flame propagation. *Twenty-Fifth Symposium (International) on Combustion/The Combustion Institute.* **25**, in press.

KERSTEIN, A. R., ASHURST, WM. T. & WILLIAMS, F. A. 1988 Field equation for interface propagation in an unsteady homogeneous flow field. *Phys. Rev. A.* **37**, 2728.

LIÑÁN, A. & WILLIAMS, F. A. 1993 *Fundamental Aspects of Combustion.* Oxford Univ. Press.

LUND, T. S. & ROGERS, M. M. 1994 An improved measure of strain rate probability in turbulent flows. *Phys. Fluids.* **6**, 1838-1847.

PETERS, N. 1992 A spectral closure for premixed turbulent combustion in the flamelet regime. *J. Fluid Mech.* **242**, 611-629.

RUETSCH, G. R. & MAXEY, M. R. 1992 The evolution of small-scale structures in homogeneous isotropic turbulence. *Phys. Fluids A.* **4**, 2747.